ELSEVIER

Ceramics International 29 (2003) 641–653

CERAMICS INTERNATIONAL

www.elsevier.com/locate/ceramint

Heat and mass transfer models in convection drying of clay slabs

Aleksandra Sander*, Darko Skansi, Nenad Bolf

Faculty of Chemical Engineering and Technology, University of Zagreb, 10000 Zagreb, Maruliæev trg 20, Croatia

Received 2 September 2002; received in revised form 30 September 2002; accepted 12 October 2002

Abstract

Drying kinetics data for convection drying of industrially prepared roof tile clay slab were approximated with different mathematical models. Applied conventional model analysis enables evaluation of main transport properties: effective diffusion coefficient, mass and heat transfer coefficients, thermal conductivity, drying constant, and exponential model parameters. A neural network-based drying model was established using backpropagation algorithm for dynamics modelling of moisture content and temperature of thin clay sample. Obtained results confirm the assumption that both, the heat and mass transfers, are under external conditions. Very small values of Biot numbers confirm that fact. Drying air temperature and initial moisture content of clay strongly influence the drying kinetics and transport properties. The dependence between the drying air temperature and evaluated transport properties shows an exponential trend. Tomas and Skansi exponential model parameter, n, is independent from temperature. At lower values of initial moisture content of clay higher drying rates are achieved, which results with higher values of calculated transport properties. It was shown that neural network as an alternative method has potential for modelling the drying process and predicting drying dynamics based on experimental data.

Keywords: A. Drying; C. Thermal properties; D. Clay; Kinetics

1. Introduction

The separation of liquid from a moist material may be carried out in a rough mechanical manner, without phase change, or by heat supply, i.e. thermal drying. Thermal drying is an important thermal separation technique used in most technical fields, for example pharmaceutical, foodstuff, ceramics, and paper industries. Heat may be supplied to a wet material by conventional heating methods (convection, conduction, radiation) or high frequency heating. Among many drying processes, convection drying is mostly used[1].

Due to different properties associated with different moist product, it follows that there are many process variations and dryer designs. In the thermal drying processes, heat and mass are simultaneously transferred. The course and time of drying process depend on drying conditions, on temperature and moisture profiles developed during the drying process, and above all, on moisture movement in the material. Moisture movement is governed by the properties, form and size of the product and the type of moisture bond in the material. Mathematical modelling of the drying process is very difficult or impossible due to the different and changing states of the moist product during drying. To date, no uniform design concept for dryers exists.

Drying is a complex process involving simultaneous heat, mass and momentum transfer phenomena, and the effective models are necessary for process design, optimisation, energy integration, and control. The development of mathematical models to describe the drying processes has been the topic of many research studies for several decades. Presently, more and more sophisticated drying models are becoming available, but a major question that still remains is the measurement or determination of the parameters used in the models. The estimation of necessary parameters should be feasible and practical for general applicability of the drying model [2].

For detailed description of the drying process, except knowing the drying kinetics, it is necessary to determine the influence of altering process conditions on essential process parameters (drying rate, process duration,

* Corresponding author. Tel./fax: +385-1-459-7259.
E-mail address: asander@fkit.hr (A. Sander).

0272-8842/03/$30.00
doi:10.1016/S0272-8842(02)00212-2

Nomenclature

Symbols

a	thermal diffusivity, $m^2\ s^{-1}$
Bi	Biot number
d	pore diameter, m
D_{eff}	effective moisture diffusion coefficient, $m^2\ s^{-1}$
h_H	heat transfer coefficient, $W\ m^{-2}\ K^{-1}$
h_M	mass transfer coefficient, $m\ s^{-1}$
ΔH	latent heat of evaporization, $Jk\ g^{-1}$
k	parameter in model 2, s^{-1}
L	half thickness of a slab, m
K	drying constant, s^{-1}
n	parameter in model 2
$q(d)$	frequency of pores with diameter d
$Q(d)$	cumulative fraction of pores, %
R	drying rate, $kg\ m^{-2}\ s^{-1}$
t	time, s
T	temperature, °C
x	slab thickness, m
X	moisture content, kg_w/kg_{dm}

Greek symbols

λ	thermal conductivity, $W\ m^{-1}\ K^{-1}$
ρ	density, $kg\ m^{-3}$
σ	mean square deviation

Subscripts and superscripts

calc	calculated
dm	dry material
eq	equilibrium
H	heat
M	mass
m	material
max	maximal
s	saturation
w	water
0	initial

transport properties) [1,2]. The first step is to choose a mathematical model that describes process kinetic. The applicability of the models has to be substantiated by comparing obtained mathematical solutions with experimental results.

Developing traditional models based on first principles is typically very time-consuming, and it is difficult for achieving accurate results with them.The neural network approach provides a method to develop a dynamic model that accounts for the instabilities and unsteady-state operating conditions. To develop such a model, the moving-window network architecture is used [3]. The standard approach to the neural network modelling of time-dependent processes uses a "black box" model, which requires no previous knowledge of a system or a process. This type of model utilizes previously recorded input/output processing patterns to predict future responses to a given set of operating conditions.

The aim of this article was to test applicability of several mathematical models (conventional and non-conventional) to drying kinetics of convection drying of a thin clay plate. The influence of air temperature and initial material moisture content on the drying kinetics, transport properties and exponential model parameters were also examined.

2. Theory

Drying data, time varying moisture content and temperature of the material were approximated with several conventional (thin-layer equations, Fick's and Fourier' equations) and one non-conventional (neural network-based) model.

2.1. Conventional mathematical models

Mathematical models usually describe drying kinetics that involve transport properties as model parameters.

The so-called thin-layer equation [2,4,5] has the following form (Model 1):

$$\frac{dX}{dt} = -K\cdot(X - X_{eq}) \tag{1}$$

In this equation K, s^{-1} is drying constant, and is the most suitable quantity for purposes of design and optimisation of drying process.

Page [4] and Tomas and Skansi [6,7] added an exponent n to time, to more precisely describe changes in the experimental data (Model 2):

$$\frac{dX}{dt} = -k\cdot n\cdot t^{(n-1)}\cdot(X - X_{eq}) \tag{2}$$

where k and n are parameters influenced by the process conditions, material properties and dominant transfer mechanism.

A third mathematical model used for approximation of experimental data is based on Fick's equation of unsteady-state diffusion [2,8]:

$$\frac{\partial X}{\partial t} = \nabla(D_{eff}\nabla X) \tag{3}$$

The solution of Fick's equation for a slab is obtained assuming constant diffusivity and convection boundary condition (Model 3):

To determine resistances of heat transfer (thermal diffusivity, heat transfer coefficient) II Fourier's law [9,10] is used (Model 4):

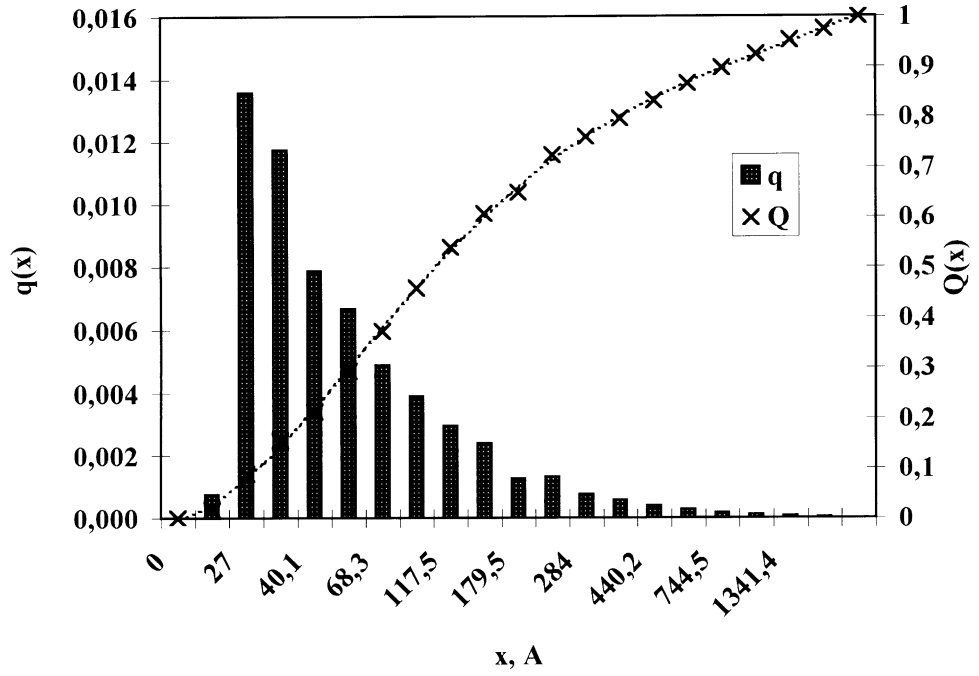

Fig. 1. Pore size distribution (histogram and cumulative plot).

$$\frac{\partial T}{\partial t} = \nabla(a\nabla T) \tag{4}$$

The transport properties (effective diffusion coefficient, mass and heat transfer coefficients, thermal conductivity) and drying constants are estimated as parameters of the selected mathematical models [Eqs. (1)–(4)] by fitting them to experimental data.

Proposed model parameters are determined by regression analysis. To test fitting of experimental data to the model, the mean square deviation has been used.

$$\sigma_X = \frac{1}{n}\sum_i \left(\frac{X_{i,\mathrm{calc}} - X_i}{X_i}\right)^2$$

$$\sigma_T = \frac{1}{n}\sum_i \left(\frac{T_{i,\mathrm{calc}} - T_i}{T_i}\right)^2 \tag{5}$$

Criterion for determination of controlling mechanism of mass and heat transfer was Biot number [2,9]:

$$Bi_M = \frac{h_M x}{D}$$

$$Bi_H = \frac{h_H x}{\lambda} \tag{6}$$

Given boundary conditions (Model 1 and Model 4) assumed that there are significant external resistances to heat and mass transfer. If Biot number is smaller than 0.1, the drying process is externally controlled [2,9,10], which means that internal resistance to mass and heat transfer is negligible. In the case of porous materials with large pores and for thin plates, the condition $Bi < 0.1$ is often fulfilled. At small Biot numbers the surface temperature and the moisture content differs little from the temperature and the moisture content in the centre of the slab. This results in uniform distribution of temperature and moisture across the slab.

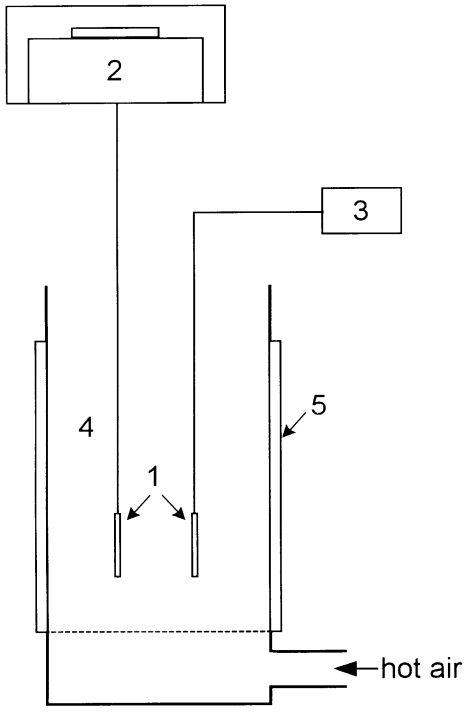

Fig. 2. Scheme of the laboratory test device for convective drying: 1—samples; 2—digital balance; 3—digital thermometer; 4—dryer chamber; 5—insulation.

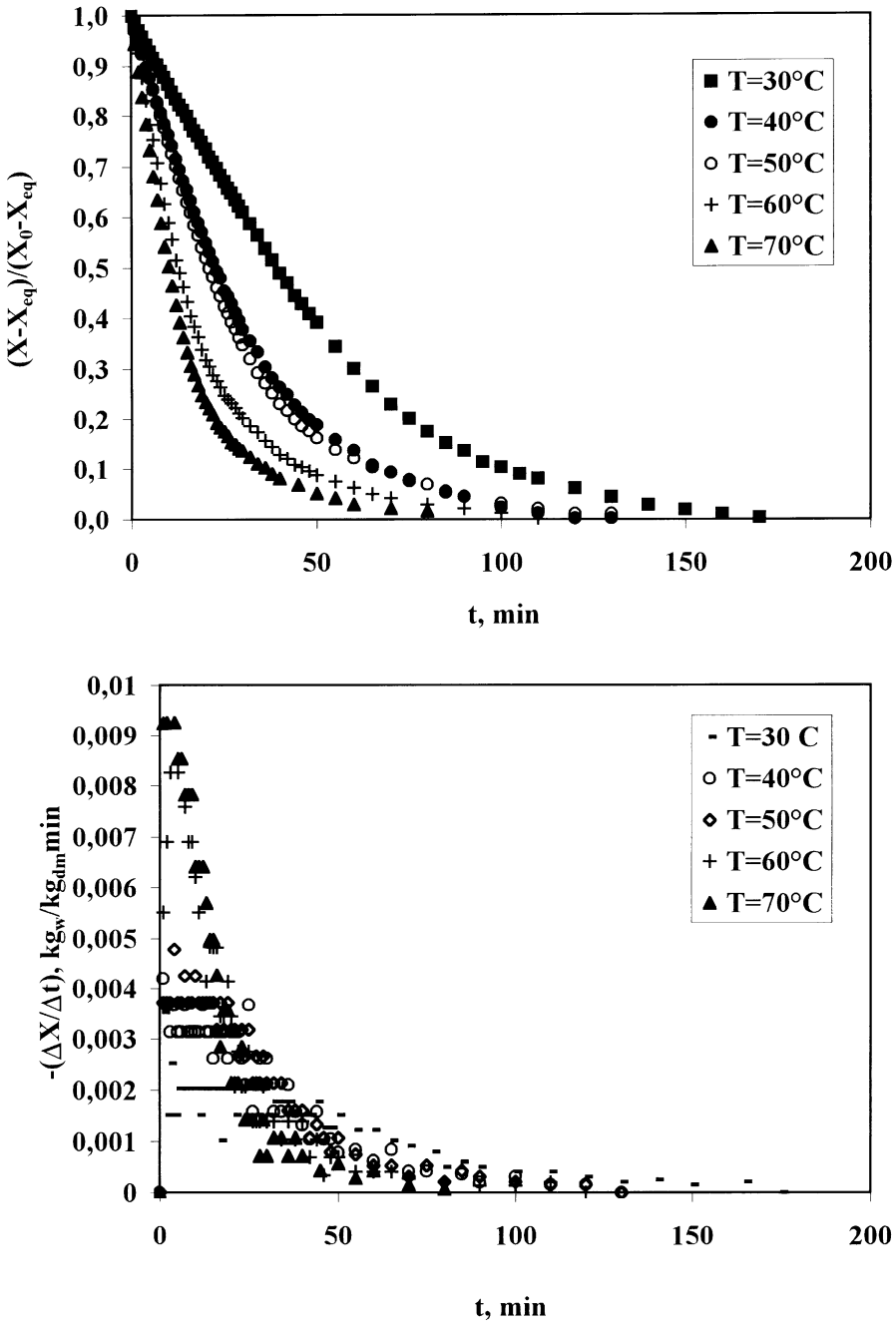

Fig. 3. The influence of air temperature on drying kinetics of clay at constant initial moisture content ($X_0 = 0.18$ kg_w/kg_{dm}).

2.2. Neural network application

The undertaken experimental research served as a base for the application of recurrent neural network, having purpose in its utilisation for modelling of drying process dynamics. The network was trained using back-propagation algorithm applying cascade learning by use of genetic algorithm in the building of hidden layer structure [11]. The number of hidden nodes was optimized to achieve the best possible performance.

Cascade learning algorithm starts off with no hidden process elements, only connection are direct connections from the input layer (and the bias) to the output layer; hidden units are added one a time. Purpose of each new hidden unit is to predict the current remaining output error in the network. Hidden process elements (PE) receive input from all previous hidden process elements as well as from the input buffer; in other words, the hidden layer has cascade connection.

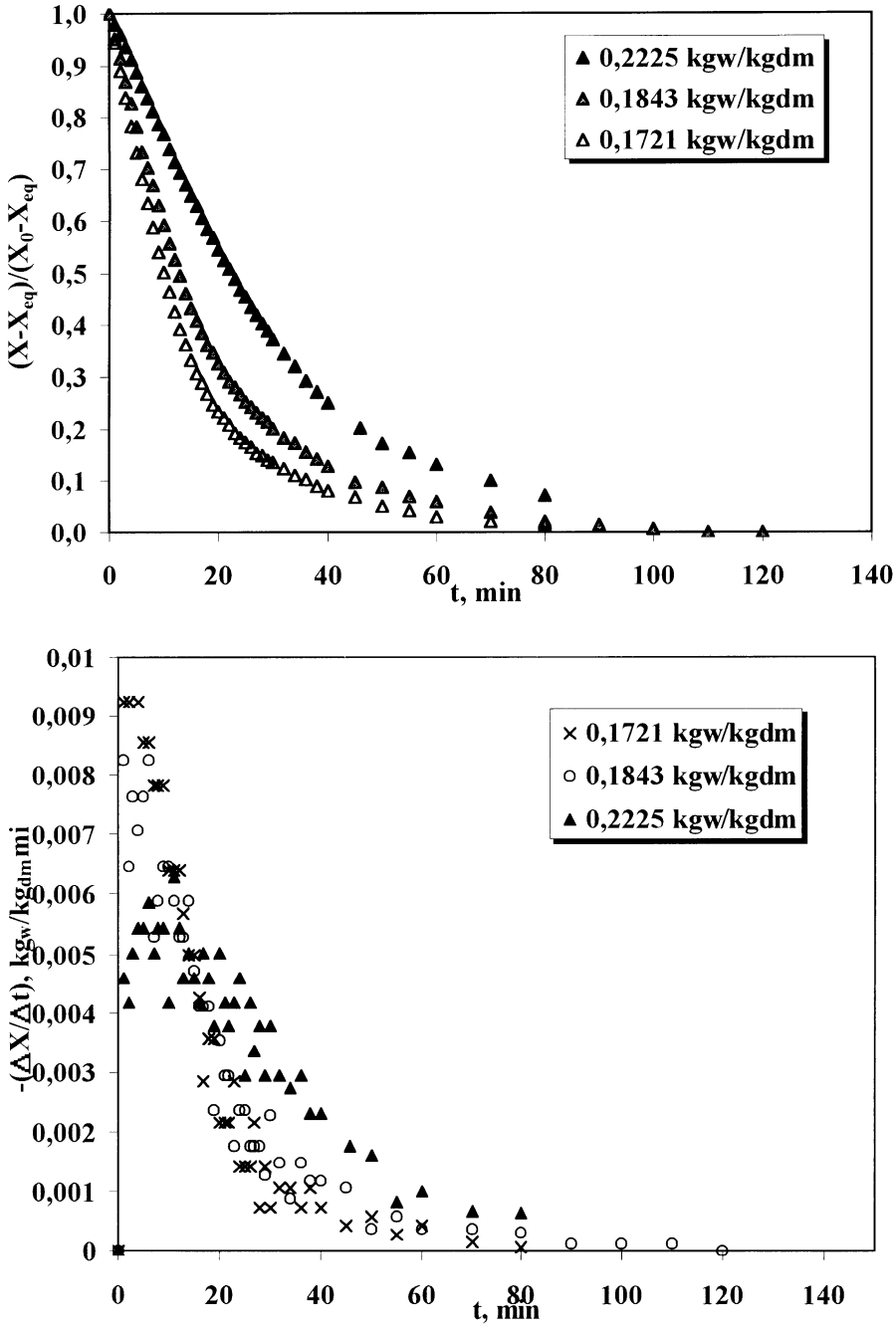

Fig. 4. The influence of initial moisture content of the material on drying kinetics of clay at constant air temperature ($T = 70$ °C).

3. Materials and methods

3.1. Materials

Material used in the experimental measurements was an illite-montmorillonite clay ($\rho = 2278$ kg/m^3) containing the quartz, kaolin, feldspat and iron hydroxides. Thin 65×55×2 mm plates (slabs) were cut of from a raw industrially shaped, flat roof tile. Initial moisture ratio was 18%–22% (wet basis).

The clay gives 1.4–6.1% of the residue on a sieve of 10^4 holes/cm^2, and 30% of particles are less than 2 μm. The drying shrinkage 7–8%, which points to the significant sensitiveness of that clay while drying [12].

Pore size distribution has been determined by nitrogen adsorption within the material by ASAP 2000 system. Pore size analysis gives cumulative adsorption surface area of 32.46 m^2/g, cumulative adsorption pore volume of 0.05276 cm^3/g, micropore volume of 0.000867 cm^3/g, and average pore diameter of 65.013 A.

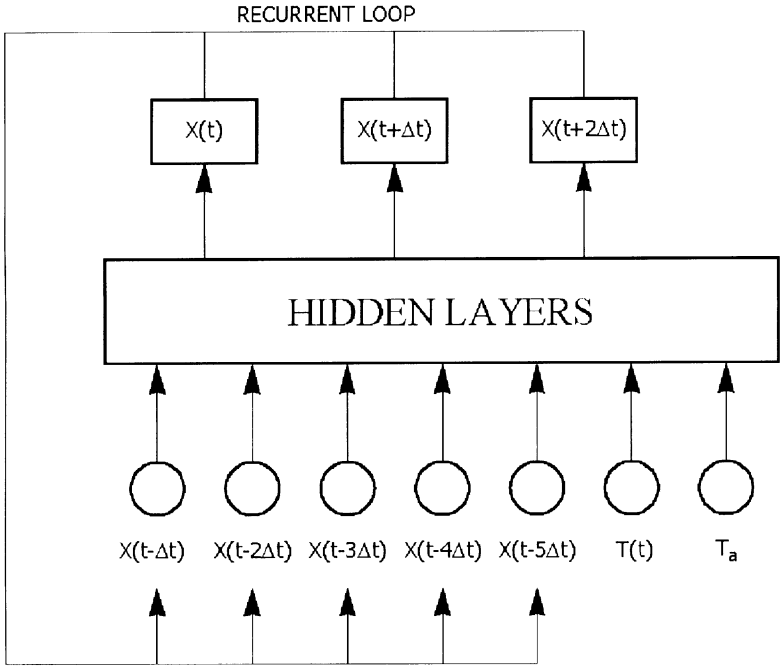

Fig. 5. Applied recurrent neural network architecture for moisture content.

Porosity of dry illite-montmorillonite clay was $\varepsilon = 0.11$. Pore size distribution is given in Fig. 1.

Equilibrium material moisture content at given temperatures was determined from the sorption isotherms evaluated by Tomas [12].

3.2. Experimental setup

Measurements were carried out in the convective drier shown in Fig. 2. The superficial air velocity had a constant value of 0.43 m/s with the relative humidity of 67%.

There were 20 experiments carried out at various temperatures (30, 35, 40, 45, 50, 55, 60 and 70 °C). Material samples had different initial moisture contents from 0.17 up to 0.25 kg_w/kg_{dm} . The mass and temperature change of the wet sample were measured continuously during the drying process. Two identical samples were used in order to measure the mass and temperature during the drying process.

Table 1
The parameters of the neural network performance

	Avg. Abs.	Max. Abs.	RMS
$X(t)$			
All	0.00112	0.0118	0.0017
Train	0.00114	0.0115	0.0018
Test	0.00105	0.0118	0.0016
$T(t)$			
All	0.272	2.77	0.495
Train	0.287	2.77	0.535
Test	0.238	1.53	0.385

It was shown earlier, even for a sample with dimensions 138×65×16 mm, that there is no temperature gradient within the material [12].

4. Results

In order to determine the transport properties and the most appropriate mathematical model, the drying kinetics of the illite-montmorilonite clay were analysed

Table 2
Calculated (Tomas and Skansi model) and measured values of maximum drying rate and critical time

T, °C	30	40	50	60	70
$(dX/dt)_{max,calc}$, kg_w/kg_{dm}min 10^{-3}	2.22	3.67	4.95	6.25	8.76
$(dX/dt)_{max,exp}$, kg_w/kg_{dm}min 10^{-3}	1.99	3.15	4.17	5.69	9.25
$t_{c,calc}$, min	14	9	5	5	3
$t_{c,exp}$, min	30	23	17	7	4

Table 3
Mass and heat transfer resistances

T, °C	Mass transfer resistance		Heat transfer resistance	
	$1/h_M \times 10^{-6}$, s/m	$L/D_{eff} \times 10^{-4}$, s/m	$1/h_H$, m^2K/W	L/λ, m^2K/W
30	3.07	6.49	3.623	0.0244
40	2.42	5.99	2.949	0.0204
50	1.83	1.17	2.262	0.0156
60	1.47	0.94	1.786	0.0126
70	1.27	0.43	1.504	0.0106

on the laboratory scale. Transport properties (effective diffusion coefficient, thermal conductivity, heat and mass transfer coefficients, drying constant, parameter k and n) were determined from experimental data, as parameters of proposed conventional models.

The influence of drying air temperature and initial moisture content on drying kinetics of convective drying of clay are shown on Figs. 3 and 4. Since the initial moisture content varies a little (for a given initial value) the time dependent moisture content curves are presented in a normalised form. Increase of hot air temperature results in steepest functional dependence $(X(t)-X_{eq})/(X_0-X_{eq})$ (higher drying rates), reducing the drying time, for a given initial moisture content. At lower temperatures existence of the constant drying rate period is visible. This period is longer for lower temperatures. For experiments carried out at temperatures higher than 60 °C, the constant drying rate period does not longer exist, because the process reaches its maximum drying rate for a very short time (3–6 min),

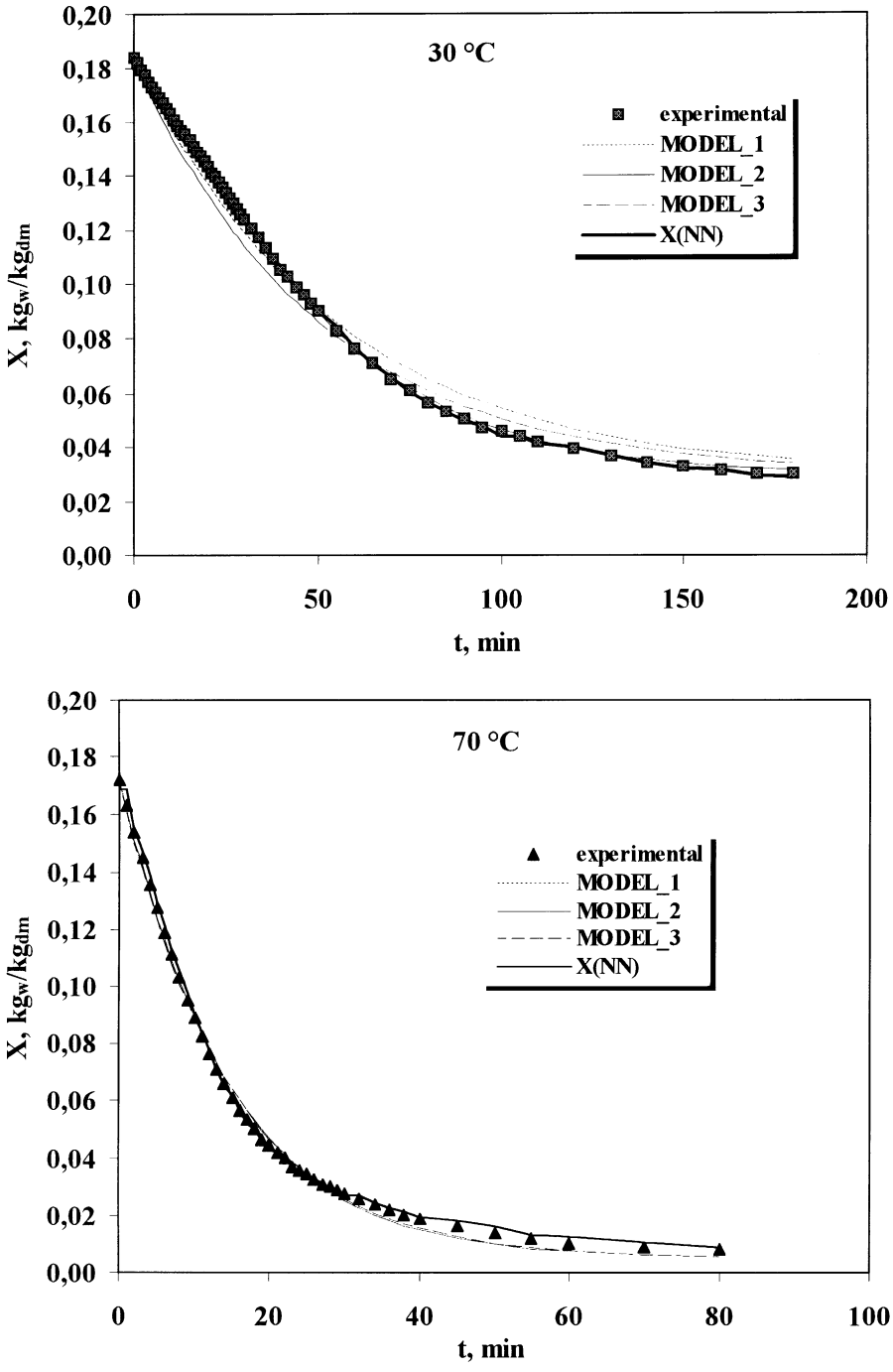

Fig. 6. Aproximation of experimental data, $X(t)$, with proposed mathematical models ($X_0 = 0.18$ kg_w/kg_{dm}).

and then its rate exponentially decreases. Since initial moisture content affects the drying kinetics, experiments were performed at three different initial moisture contents. When initial moisture content is lower, the maximal drying rate is higher and drying time is reduced.

The neural network input layer includes the initial moisture content, X_0, the temperature of the air stream, T_a, and the time-dependent variable: the moisture content in the last five time steps, $X(t-\Delta t),\ldots,X(t-5\Delta t)$, and the sample temperature in the last five steps, $T(t-\Delta t),\ldots,T(t-5\Delta t)$. The output layer includes predicted future moisture content and the temperature sample during the drying process. Prior to building the network, data that will be used for network training, and testing have been selected. The neural network has afterwards been built within hidden layers by adding hidden nodes. Final network architecture, which has

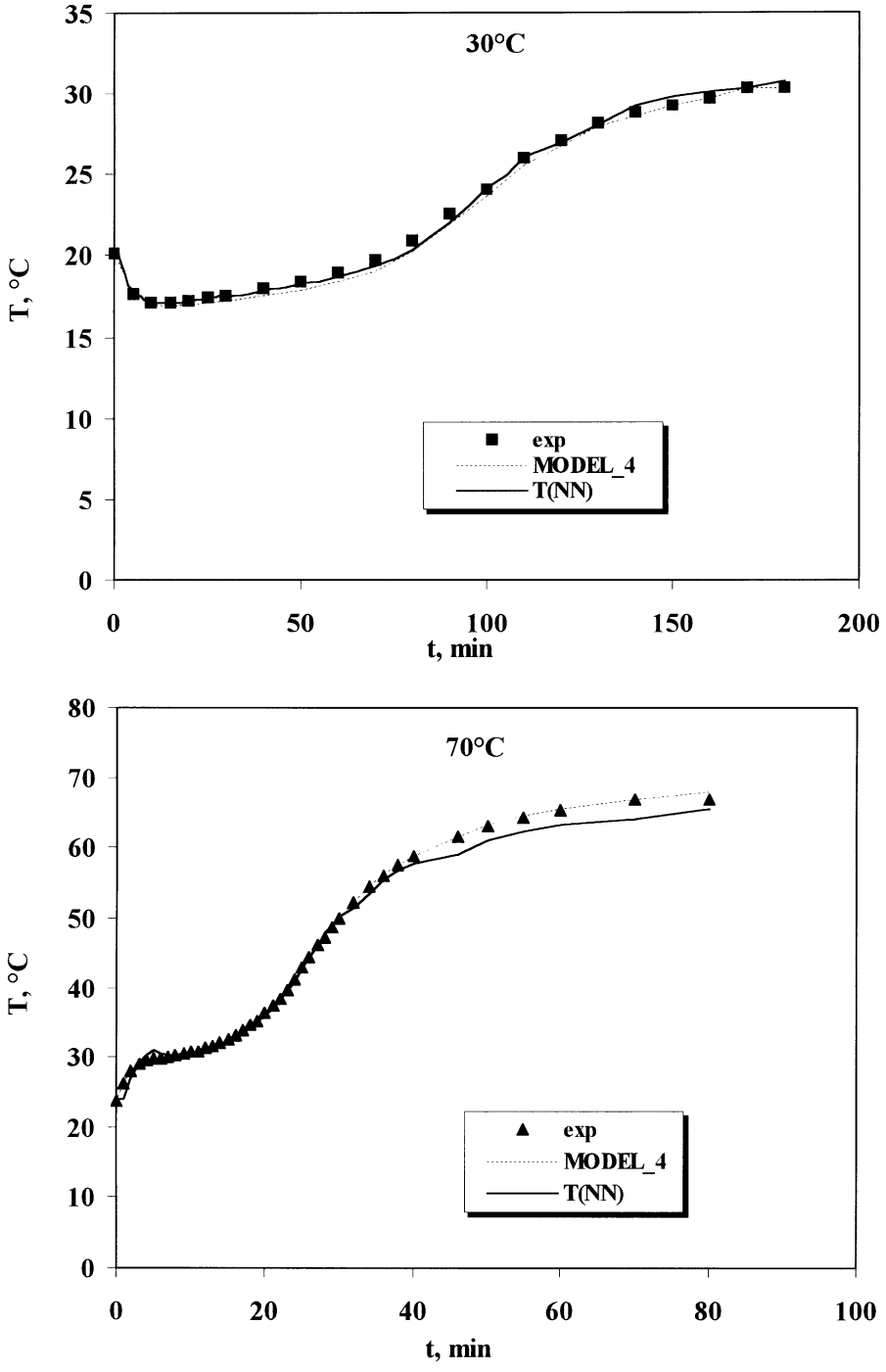

Fig. 7. Aproximation of experimental data, $T(t)$, with proposed mathematical models ($X_0 = 0.18\ kg_w/kg_{dm}$).

been built by adaptive gradient learning algorithm with sigmoid transfer function, has one hidden layer consisting of eight nodes. The network structure for dynamic modelling of moisture content is shown in the Fig. 5. The neural network for prediction of sample temperature has a similar structure. Finally, the network performance was tested. After network constituting and training, its work has been checked using previously selected testing data sets. This procedure has been undertaken using NeuralWare software package 'Predict' and ProfII/Plus.

All the measures in Table 1 are calculated on the real world target outputs. Avg. Abs. is the average absolute error between the target output and the prediction. RMS is the root mean square error between the target output and the prediction. Finally, the neural network-based model was compared with obtained data using conventional models.

As mentioned earlier, all applied mathematical models involve material equilibrium moisture content so its values were determined by means of sorption isotherms for a given material.

In order to find out which of applied models better correlates experimental data, parallel survey of measured and calculated data (conventional and nonconventional models), for initial moisture content of about 0.18 kg_w/kg_{dm}, is show in Fig. 6. The best correlation for mass transfer is achieved with the neural net-

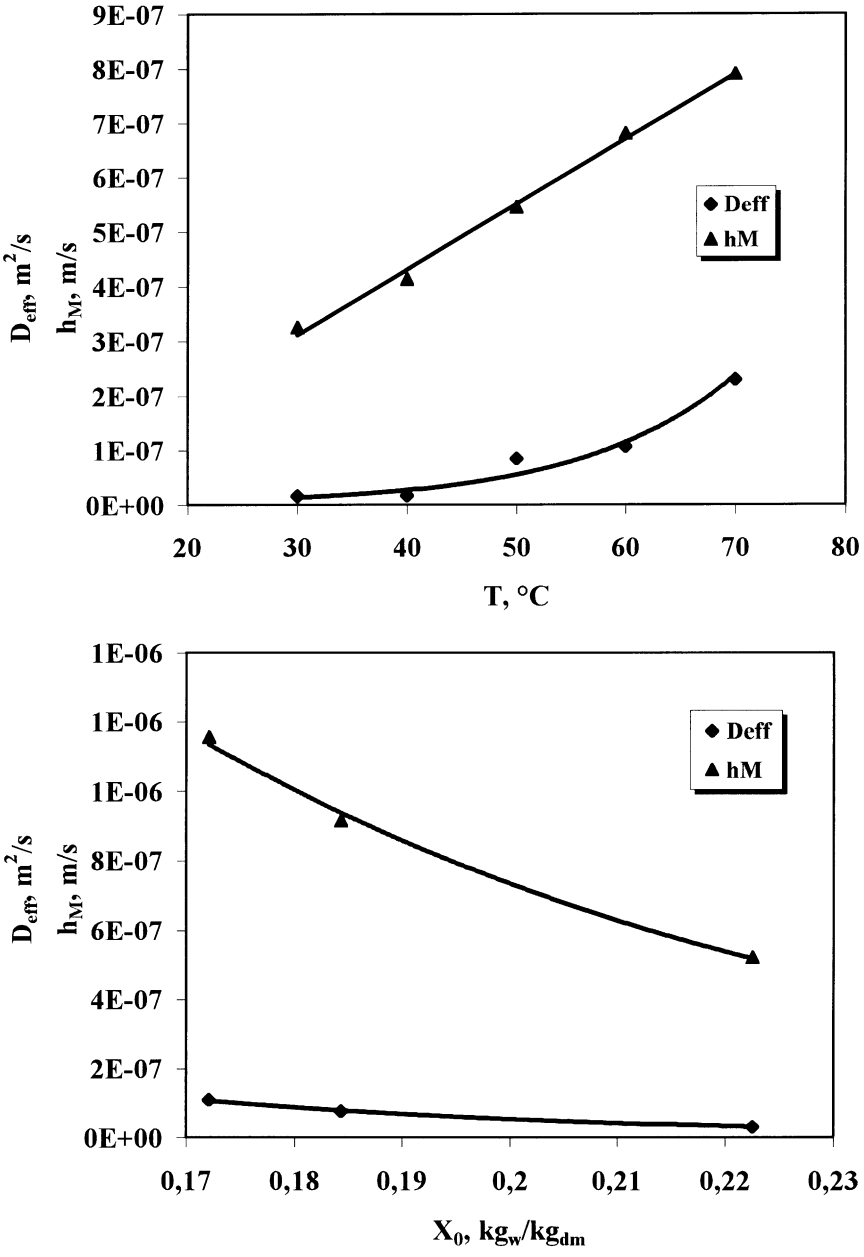

Fig. 8. The influence of drying conditions on effective diffusion coefficient and mass transfer coefficient.

work based model, even though all models are compatible with the experimental data. The mathematical model, $T(t)$, for heat transfer also correlates highly with measured material temperature (Fig. 7). Deviation between measured and calculated data for all conventional models is higher at lower process temperatures. This can be explained with non-existence of a constant rate period at higher temperatures. Concerning the type of proposed conventional mathematical models (exponential), the differential form of those equations cannot indicate the existence of a constant rate period (equations has one maximum). That results in slight differences between calculated (Tomas and Skansi model) and experimental values (Table 2).

Since properties and behaviour of materials during drying depend on porous material structure, the pore size distribution of illite-montmorilonite clay was determined. As mentioned earlier, the micropore portion is negligible. This fact was taken into account when boundary conditions were defined. As expected, the drying process is governed by the external resistances to heat and mass transfer (because of the inner pore structure and sample geometry—thin plate). Obtained Biot numbers, for both mass and heat transfer, are very small (Bi_M ranges from 3.42×10^{-3} to 2.12×10^{-2}; Bi_H from 1.4×10^{-4} to 1.5×10^{-4}). The surface temperature and moisture content differ little from their values at the centre of the slab, so temperature and moisture dis-

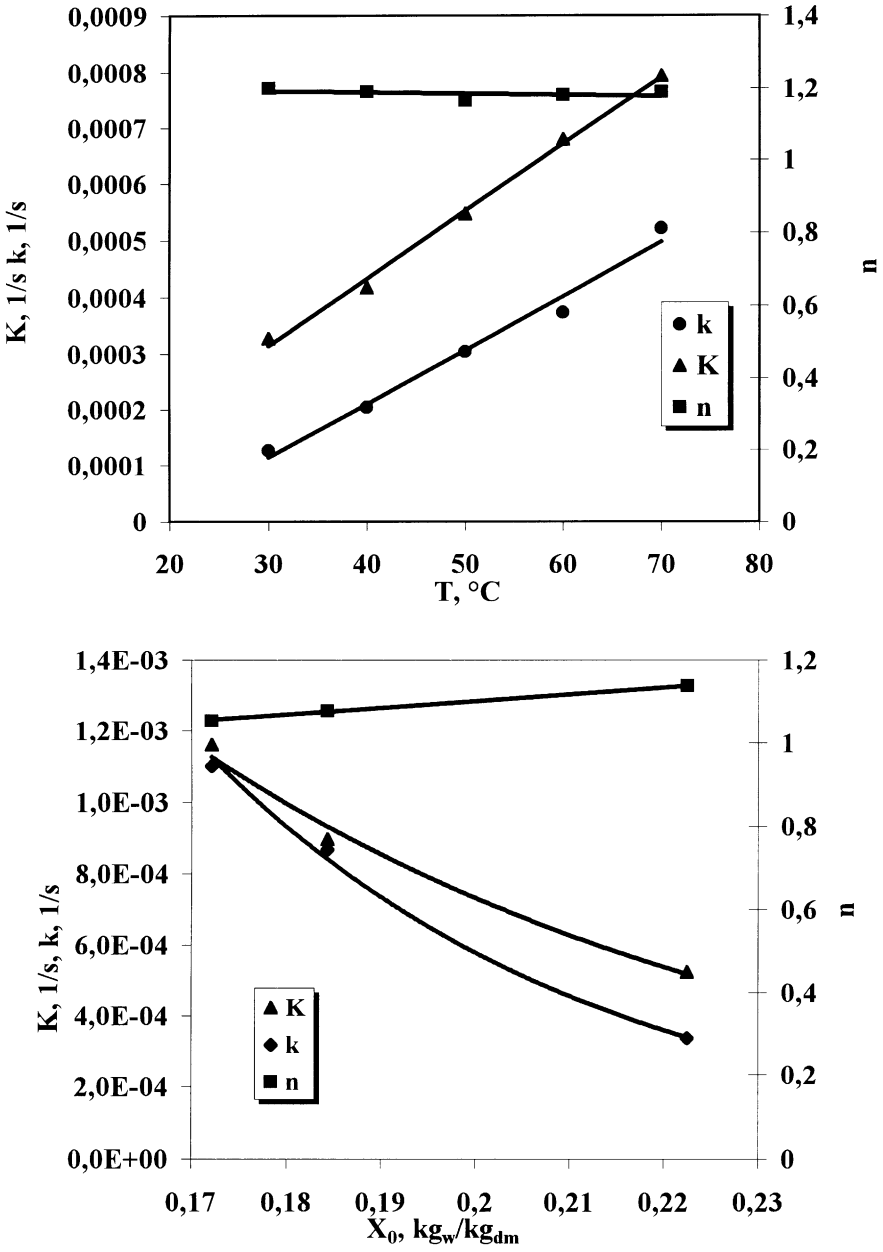

Fig. 9. The influence of drying conditions on drying constant and parameters k and n.

tribution across the material is uniform. The rate of heating and dehumidification depend only on the intensity of heat and mass transfer at the solid/air interface, so the process of mass and heat transfer is externally controlled. To substantiate that, resistance to heat and mass transfer are shown in Table 3. It can be seen that external resistances, $1/h_M$ and $1/h_H$, are much larger than internal resistances, L/λ and L/D_{eff}.

The influence of drying air temperature and initial moisture content of material on approximated values of transport properties, parameters k and n, and maximum drying rate are presented in Figs. 8–11. The increase of temperature, for a given initial moisture content, causes an exponential increase of the effective diffusion coefficient, thermal conductivity, heat transfer coefficients and parameter k, while the mass transfer coefficient and

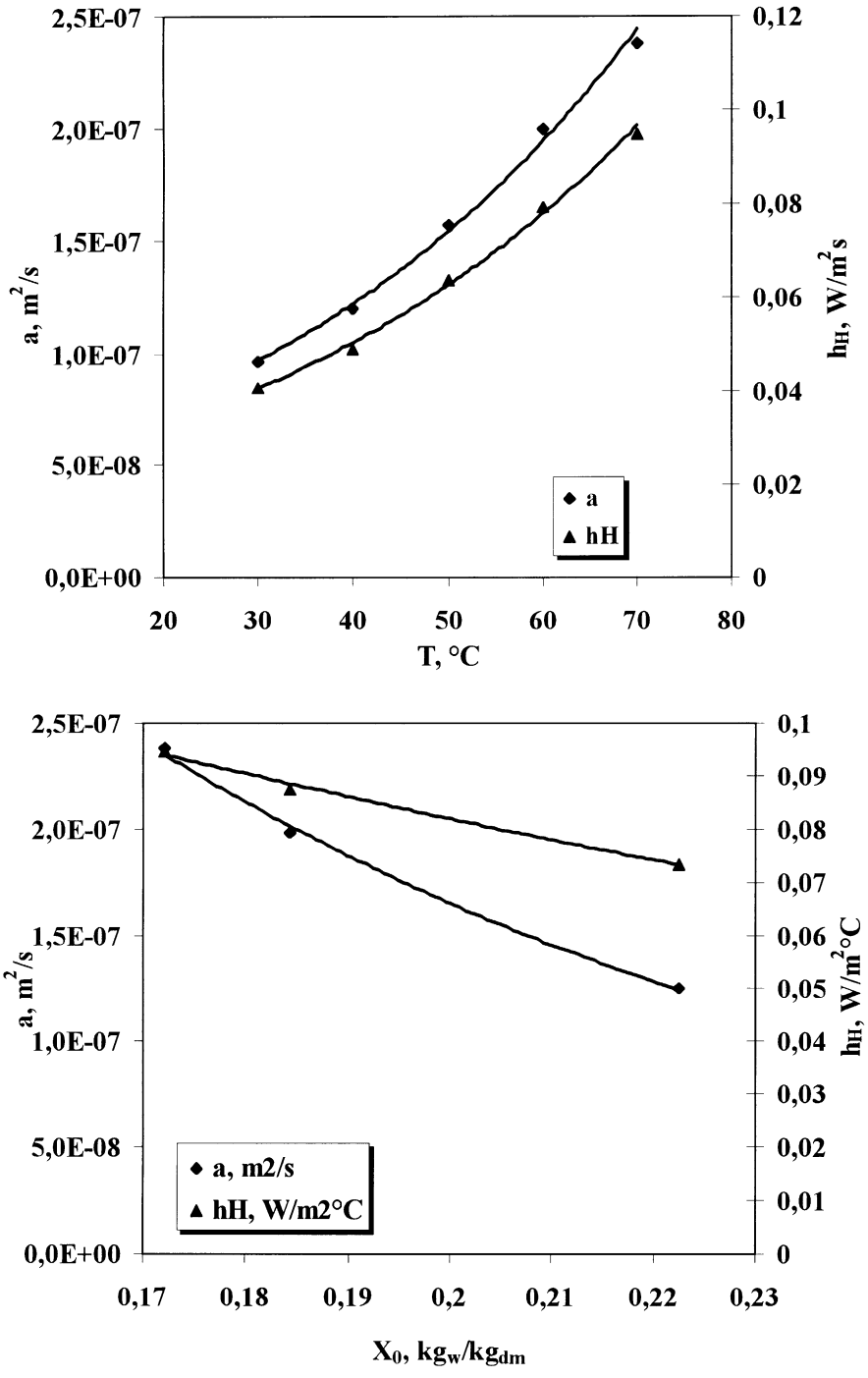

Fig. 10. The influence of drying conditions on thermal diffusivity and heat transfer coefficient.

drying constant increases linearly. Parameter n is independent of temperature.

Exponential dependencies of the above parameters are probably caused by the exponential temperature dependence of vapour pressure inside the material (Antoine Reid correlation). It was shown earlier that parameter n value depends on the way that heat is supplied to a material (drying method) [13]. The maximum drying rate also increases exponentially with temperature, while critical time (the beginning of falling rate period) decreases. Similar relations were obtained when the influence of initial moisture content on evaluated parameters were analysed. Higher values of transport properties, Tomas and Skansi model parameter k and maximum drying rate were achieved at lower initial moisture contents. Initial moisture content slightly affects Tomas and Skansi model parameter n (exponent on drying time).

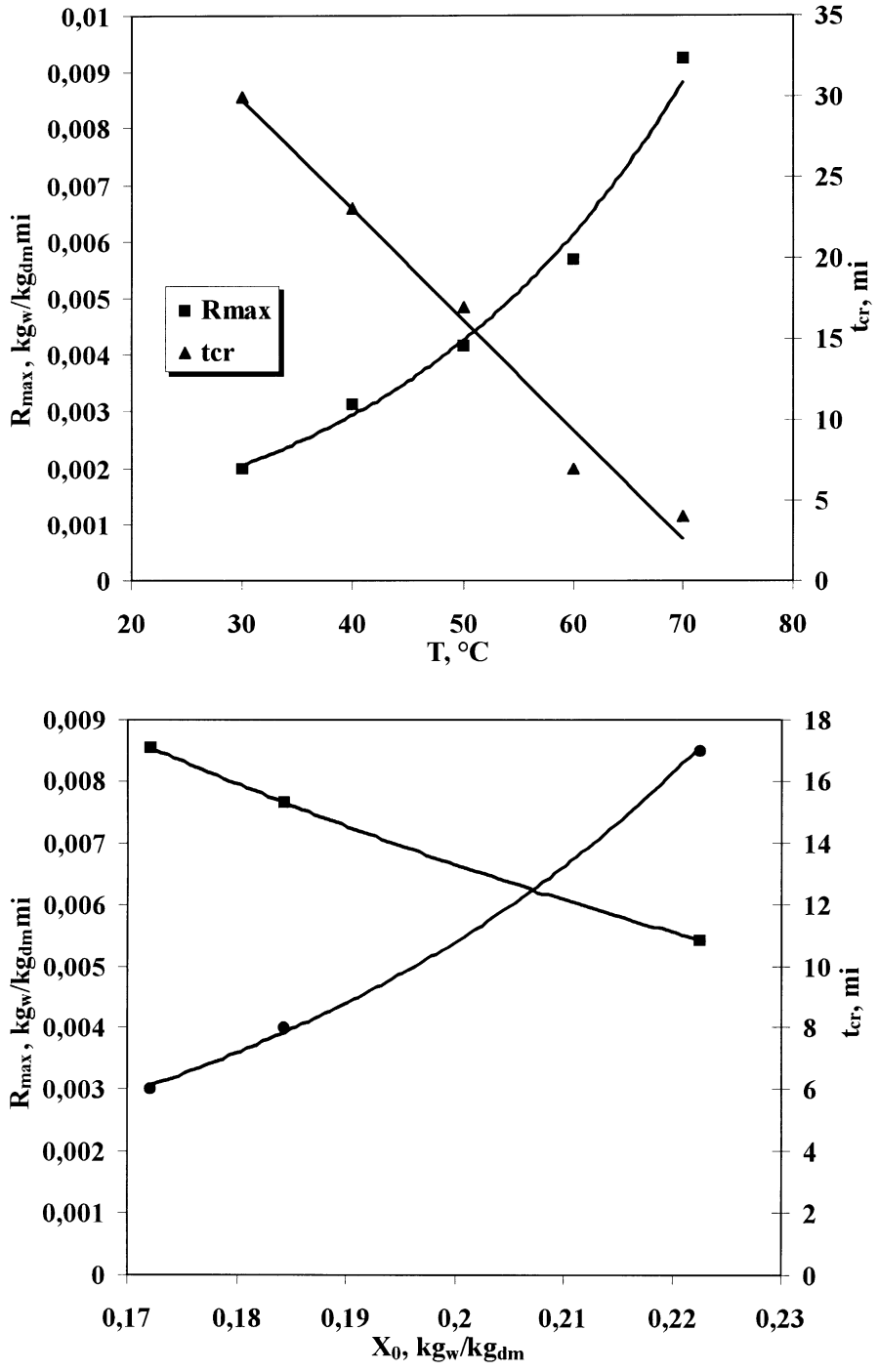

Fig. 11. The influence of drying conditions on maximum drying rate and critical time.

5. Conclusion

This paper argued conventional mathematical models, and a neural network-based model in describing the drying kinetics of thin industrially prepared clay plate, in isothermal conditions.

Effective diffusion coefficient, mass and heat transfer coefficients, thermal conductivity, drying constant, and exponential model parameters in isothermal condition, being the main transport properties of thin clay plate were approximated, and correlated with drying conditions (drying temperature and initial moisture content).

The influence of air temperature, and initial material moisture content on the drying kinetics, transport properties and exponential model parameters were analysed. Increase in temperature causes increase of all the coefficients, except for exponential model parameter, n, that is independent of temperature. Higher values of transport properties, Tomas and Skansi model parameter k and maximum drying rate were achieved at lower initial moisture contents. Initial moisture content slightly affects Tomas and Skansi model parameter n (exponent on drying time).

Very small Biot numbers, less than 0.1, for both heat and mass transfer, indicate that the heat and mass transfer are under external conditions.

Good fitting between experimental results and process models has been found.

References

[1] K. Sattler, H.J. Feindt, Thermal Separation Processes, VCH, Wienheim, 1995.
[2] A.S. Mujumdar, Handbook of Industrial Drying, Marcel Dekker, New York, 1995 (Part 1).
[3] D.R. Baughman, Y.A. Liu, Neural Networks in Bioprocessing and Chemical Engineering, Academic Press, San Diego, 1995.
[4] D.S. Jayas, et al., Review of thin-layer drying and wetting equations, Drying Technology 9 (3) (1990) 551–588.
[5] S. Sokhansany, S. Genkowski, Equipment and methods of thin-layer drying: a review, in Proc. 6th Inter. Drying Symp. (IDS 1988), France '88, pp. 159–170.
[6] S. Tomas, D. Skansi, M. Sokele, Kinetics of the clay roofing tile convection drying, Drying Technology 11 (6) (1993) 1353–1369.
[7] A. Sander, S. Tomas, D. Skansi, The influence of air temperature on effective diffusion coefficient of moisture in the falling rate period, Drying Technology 16 (7) (1998) 1487–1499.
[8] J. Cranck, The Mathematics of Diffusion, Clarendon Press, Oxford, 1956.
[9] V.P. Isachenko, V.A. Osipova, A.S. Sukomel, Heat Transfer, MIR Publishers, Moscow, 1977.
[10] L.E. Sissom, D.R. Pitts, Elements of transport phenomena, McGraw Hill Book Company, New York, 1972.
[11] Neural Computing, A Technology Handbook for Professional II/PLUS and NeuralWorks Explorer, NeuralWare, Inc, Pittsburgh, 1996.
[12] S. Tomas, Untersuchung der Trockungskinetik der Ziegelerzeugnisse, Master Thesis, University of Zagreb, Zagreb, Croatia, 1988.
[13] J. Prlic Kardum, A. Sander, D. Skansi, Comparison of convective, vacuum and microwave drying of chlorpropamide, Drying Technology 1 (19) (2001) 169–185.